Reference: *Biol. Bull.* **214:** 99–110. (April 2008)

Structural and Functional Changes in Regenerating Antennules in the Crayfish *Orconectes sanborni*

JULIANNE ROSE MCCALL AND KRISTINA STAFFORD MEAD*

Biology Department, Denison University, Granville, Ohio 43023

Abstract: Crayfish rely on the chemosensory neurons in their antennules to help them find food and habitat and to mediate social interactions. These structures often sustain damage from aggressive interactions or from the environment, but they have the ability to regenerate. In this study, we examine whether the effects of antennule ablation and regeneration on odor-tracking ability correlate with structural changes in the antennule that occur during regeneration. We initiated the regeneration process by removing the right antennules from 55 individuals of *Orconectes sanborni*. We developed a method to nondestructively sample the regenerating antennules so that we could follow the growth of new antennular tissue in the same animals over time. We used dental epoxy to make molds of the regenerating antennule after each molt. We then made resin positives, which were visualized using scanning electron microscopy. Structural parameters including aesthetasc length, diameter, segment length, and number per row were measured from scanning electron micrographs using Image J software. Crayfish were tested in a tabletop water Y-maze before and after surgery and after each molt to assess their ability to track food odors. The structural and the behavioral data indicate that the antennules possessed many aspects of their original structure by the end of the second molt. Flicking of antennules, investigation of substrate, success rate at finding the odor-containing Y-maze branch, and time to completion of Y-maze regained pre-antennulectomy values by the end of the third molt.

Introduction

Crayfish as useful models for the study of nerve regeneration

The crayfish antennule is a useful model for the study of the characteristics and mechanisms of neural repair for many reasons. The connections between the olfactory receptors on the external structures and the olfactory lobes within the brain are structurally simple and are modest in number of neurons (Sandeman and Sandeman, 1991). Crayfish combine a relatively long life with a high rate of regeneration throughout their life span (Skinner, 1982; Laverack, 1988; Harrison *et al.*, 2001, 2003, 2004). Crayfish fight frequently, often damaging their antennules (thus providing a stimulus for regeneration; Breithaupt, 2001). Many critical activities, including scavenging for food, seeking mates, and aggressive encounters are accomplished mainly through their keen sense of smell (Ache, 1982). These structural, ecological, and behavioral factors make crayfish a good model for the study of nerve regeneration.

Crayfish antennular olfactory structures

Crayfish detect odors from distant sources with their antennules, located medially to the antennae. Each antennule is composed of a lateral and a medial flagellum, each of which is segmented and contains up to 30 annuli (Tierney *et al.*, 1986).

Recent evidence from spiny lobsters and other crustaceans suggests that many crustaceans possess two antennular pathways that contribute to chemically mediated responses (Schmidt *et al.*, 1992; Schmidt and Ache, 1996; Mellon, 2007). In the olfactory pathway, odors from distant sources are detected by aesthetascs, which are sensilla that are chemosensory only (Hallberg *et al.*, 1992). Olfactory neurons within the aesthetascs project into the olfactory lobe (Schmidt and Ache, 1992). The non-olfactory chemoreceptive pathway involves non-aesthetasc sensilla that are mixed chemosensory and mechanosensory in function, and that project onto the lateral antennular neuropil (*e.g.,* Schmidt *et al.,* 1992*)*. The non-aesthetasc pathway is thought to mediate antennular movements, antennular grooming behavior, and other reflexes, while the aesthetasc

Received 10 May 2007; accepted 19 December 2007.

* To whom correspondence shoud be addressed. E-mail: meadk@denison.edu

pathway appears to be responsible for more complex behaviors, such as courtship behavior in male crabs (Gleeson, 1982). Detection and orientation to food odors can be mediated by either pathway in spiny lobsters (Steullet *et al.,* 2001; Horner *et al.,* 2004). The relative roles of the two pathways in crayfish are not yet known, although the aesthetasc pathway has been shown to mediate fighting behavior (Horner *et al.,* 2008). Because aesthetascs are by far the most numerous type of olfactory chemoreceptive sensilla in crayfish, and since early experiments indicate that the aesthetasc-bearing lateral flagellum of the biramous antennule is more essential for odor-tracking behavior (Dunham *et al.,* 1997; Giri and Dunham, 1999), this paper concentrates on aesthetascs.

Crayfish aesthetascs are cuticular, hairlike sensilla located on the ventral side of the distal half of the lateral flagellum (Tierney *et al.*, 1986; Sandeman and Sandeman, 1996). Adult aesthetascs are 100–150 μm long, 13–17 μm in diameter, and contain 40–110 olfactory receptor neurons (ORNs) and many supporting cells (Tierney *et al.*, 1986). The aesthetascs are organized along the adult antennule into two rows of 3–6 aesthetascs per annulus. One of the primary goals of this paper is to compare the structure and distribution of the aesthetascs before and after regeneration by making repeated structural measurements of the same antennule as it progresses through a series of molts.

Functional consequences of antennule and aesthetasc loss and regeneration

The complete ablation of one of the two antennules leaves the crayfish unable to track odors (Kraus-Epley and Moore, 2002). Removal of the aesthetasc-bearing portion of the lateral antennule flagellum causes the crayfish to lose as much of its olfactory lobe as if the entire appendage were removed, suggesting that aesthetascs are the primary olfactory sensilla (Mellon, 2000; Horner *et al.,* 2008). However, until now, there has been no study of how olfactory function is regained during regeneration, or of which structural changes enable that regained ability. Therefore, a second goal of this paper is to correlate changes in odor-tracking ability with changes in aesthetasc structure and distribution over a succession of molts in the same group of animals.

Aesthetasc addition during development and normal adult molts

Different processes seem to be steering aesthetasc insertion during the molts that occur during early development and during later adult molts. In newly hatched crayfish, aesthetascs are added uniformly along the entire outer two-thirds of the antennule (Sandeman and Sandeman, 1996). Later in development (>7 mm carapace length in *Cherax destructor*), each molt involves the addition of new aesthetascs at the proximal portion of the aesthetasc-bearing region and the shedding of the oldest aesthetascs from the distal-most region of the antennule (Mellon *et al.*, 1989; Sandeman and Sandeman, 1996). In the Caribbean spiny lobster *Panulirus argus*, translocation of a single aesthetasc from proximal to distal end takes three to six molts (Steullet *et al.*, 2000a). The number of ORNs within each aesthetasc increases only slightly throughout development (Derby *et al.*, 2003), suggesting that entire olfactory sensory units repeated along the antennule (Steullet *et al.,* 2000b) are being cycled, rather than simply the ORNs. A third question that we wish to address in our study is whether regenerating antennules in adult animals grow according to the turnover patterns seen in nonregenerative adult molting cycles, or are more like the patterns of aesthetasc insertion along the entire antennule seen in very young animals.

Functional anatomy of the crayfish antennule

For odor-tracking to be successful, odor-containing water must be able to physically penetrate the array of chemosensors on the antennule. Here, we concentrate on aesthetascs. Crayfish, like many crustaceans, typically sample their chemical environment by moving their antennules rapidly through the surrounding fluid (Snow, 1973; Schmitt and Ache, 1979; Devine and Atema, 1982; Gleeson *et al.,* 1993,1996; Hallberg *et al.,* 1997). This flicking motion typically reduces the thickness of the boundary layer coating the antennule. Work done in models inspired by similar-sized stomatopods suggests that the thinner the boundary layer, the more rapid the diffusion of odor molecules from the surrounding fluid to the surface of the olfactory sensilla (Mead and Koehl, 2000; Stacey *et al.*, 2003). Aesthetasc length can be used to determine the probable degree to which the sensors extend beyond the boundary layer created by the supporting antennule and thus better gain access to odorant molecules in the surrounding fluid.

Gap:diameter ratio

Physical and mathematical modeling of sensilla as cylinders shows that the size and spacing of the cylinders affect the thickness of the boundary layer coating the cylinders (Cheer and Koehl, 1987; Hansen and Tiselius, 1992; Koehl, 1995, 1996). A critical parameter appears to be the ratio of the gap between adjacent rows of aesthetascs and the aesthetasc diameter (gap:diameter ratio), which can be used to predict how much fluid will be able to move through the array. Similar dynamically scaled models of stomatopod aesthetascs, which are similar in dimension to crayfish aesthetascs, have shown that having sensilla too close together can inhibit the ability of the sensors to encounter odor molecules present in the surrounding fluid (Mead and Koehl, 2000; Stacey *et al.,* 2003). This close spacing can, however, prolong the presence of a given odor sample, increasing the probability of detecting a particular odor

present in the sample (Mead *et al.*, 1999, Stacey *et al.*, 2003). Other spacing parameters, such as the relative spacing of aesthetascs within a row, may also be important.

We wish to relate the effects of antennule ablation and regeneration on odor-tracking ability to the structural changes in the antennule that occur during regeneration. To that end, we antennulectomized crayfish and tested the crayfishes' chemosensory abilities in a Y-maze before and after surgery and after each molt. In parallel, we made resin copies of each animal's antennules to compare antennule and aesthetasc structure of the same animals before and after surgery and after each molt. We hypothesize that differences in Y-maze success will be reflected in structural changes at the level of aesthetascs and antennules.

Materials and Methods

Collection and maintenance of crayfish

Fifty-five individuals of *Orconectes sanborni* ranging in size from 21.9 to 57.5 mm rostrum-telson length were collected from streams in the Denison University Biological Reserve (Granville, OH). Crayfish were individually housed in containers filled with room-temperature (22–25 ^{o}C) dechlorinated water. Each crayfish was fed dry cat food.

Antennulectomies

To initiate the regeneration process, the right antennule of each crayfish was severed at the base. The excised antennules were fixed in 70% ethanol and then dehydrated in an alcohol gradient series. Samples were further dried using hexamethyldisalazane before they were analyzed using standard scanning electron microscopy protocols and the measurement methods described below. Crayfish odor-tracking behavior was tested with a Y-maze, and antennule structure was analyzed with the resin-mold method after surgery and after each molt.

Y-maze tests

Two weeks after surgery and two weeks after each molt, crayfish were tested in a water Y-maze to assess their ability to find the side of the maze containing odor (7–8 g of chicken liver in a mesh bag). The Y-maze apparatus consisted of a 1-m-long main trough and two 1-m side troughs set into the main trough at 120^{o}. During experiments, distilled water flowed into each branch at a rate of 30 ml/s and was released at the base of the maze. Straw collimators kept the flow in the working section of the maze laminar. Water depth within the maze was kept at between 4.5 and 6 cm. The floor of the maze was coated with small pebbles to keep the crayfish from slipping on the smooth plastic surface of the trough. The liver bait was placed at the end of either the right or left branch (determined randomly) of the maze. To minimize visual cues, the maze apparatus was draped in black material and room lights were turned off during each session. Each crayfish was marked with a triangle-shaped piece of reflective (3M Co.) tape to aid in digitizing its movements. The infrared feature of the videocamera made it possible to record movement without an additional light source.

A maze session was initiated by placing pre-antennulectomy, post-ablation (0th molt), 1st molt, 2nd molt, or 3rd molt crayfish at the base of the maze. Sessions were video-recorded. Crayfish odor-sampling behavior, such as flicking and investigating the Y-maze pebble substrate, was also recorded. When the crayfish walked up the baited branch to the end, it was determined to have successfully completed the Y-maze. Trials were terminated after 10 min, although no active animals took longer than 7.5 min. Trials in which the crayfish shot up the Y-maze in 10 s or less were also excluded, on the grounds that the animal appeared to be responding to a stimulus other than odor. Only runs in which a crayfish made a decision were included in the Y-maze completion data, and only data from successful trials were included in the time-to-decision data. Control trials, with no food in either arm, were also performed.

New method to study structural regeneration

Until now, detailed studies of antennule regeneration have required that the antennule be removed for analysis. The experimenter has to either start with a very large number of animals or allow animals to repeatedly regrow and sacrifice their antennules. To alleviate stress and minimize the number of animals needed for this type of study, we developed a method for nondestructive, repetitive sampling. We derived inspiration from botanical methods used to follow the fate of microscopic structures on leaves by acquiring precise surface impressions (Geisler *et al.*, 2000).

Molds of regenerating antennules were made prior to the 1st molt and after the 1st, 2nd, and 3rd molt. Crayfish were held upside-down under a dissecting scope with wax and clay. The claws, antennae, and left antennule were restrained with wax and pins. The regenerating antennule was extended from the body and was gently dried with a Kim-Wipe. Spurr's dental epoxy resin impression material was prepared by mixing approximately 150 μl of Coltène President light body polyvinylsiloxane (Whaledent C-4667) base with 150 μl of Coltène President catalyst for 45 s. Immediately after mixing, the material was placed on the prepared antennule so that the substance could surround the antennule (Fig. 1A). The material was allowed to harden for 7 min and was then slowly pulled from the crayfish (Fig. 1B). When the impression material completely surrounded the antennule, a dorsal channel was cut to expose the inner antennule groove. This method was tested with a series of control experiments on nonregenerating animals. These animals enjoyed similar Y-maze success (75%–80%, depend-

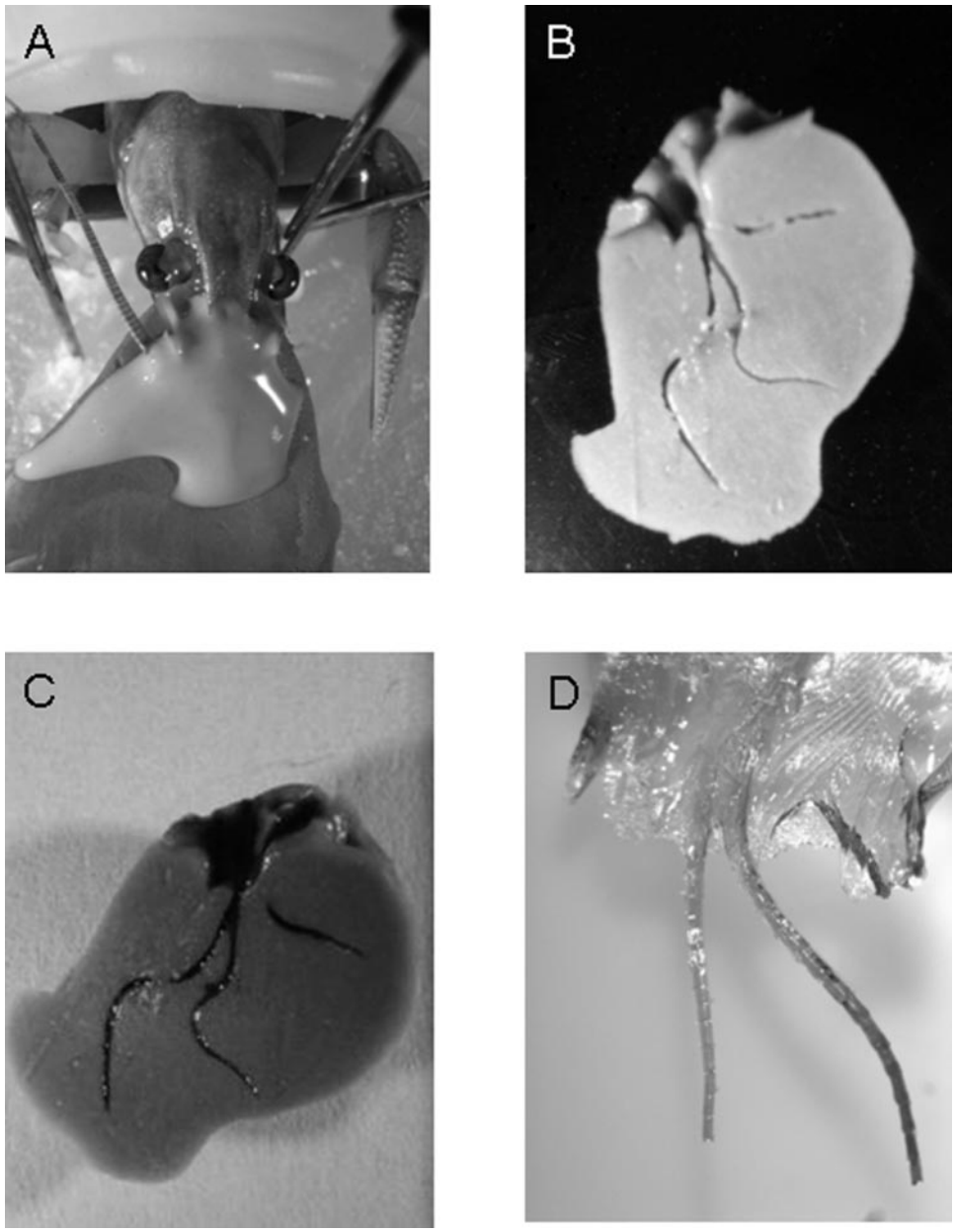

Figure 1. Making impression molds and resin positives of a regenerating antennule. (A) The impression material covers the antennules and sets for several minutes. Although this procedure is usually carried out with the animal inverted, this image shows the crayfish right-side up. (B) The product of the hardened material. (C) The epoxy resin is injected into the impressions and cured for 12 h. (D) The final product is a resin positive of the antennule that can be studied under light microscopy or scanning electron microsopy.

ing on the experiment) before and after resin impressions were made of their antennules.

Antennule resin positives

Ted Pella #18108 embedding material was prepared by thoroughly mixing 5.5 ml of noneyl succinic anhydride, 2 ml of vinylcyclohexane dioxide, 1.2 ml of Dow epoxy resin 736, and 100 μl of dimethylaminoethanol. The mixture was drawn into 23-gauge syringes and stored at 4 ^{o}C if it was to be used within 2 days, and at -20 ^{o}C for up to a month. Embedding material was warmed for 5 min at room temperature prior to slow injection into the impression molds (Fig. 1C). The resin was cured at 70 ^{o}C for 8 h, extracted from the impression molds (Fig. 1D), and mounted on Pella SEM stubs covered with carbon-conductive adhesive tabs (Ted Pella 16084-3).

Scanning electron microscopy

Stub-mounted original antennules and resin positives were coated in a 20-nm layer of palladium-gold alloy (Pelco model 3 sputter coater 91000). Images were taken with a 15 kV beam using a Philips XL30 scanning electron microscope. Slight pixel shape changes caused by the file compression process were removed using a program (Xlstrtch.exe) distributed by Philips.

Antennule measurements

Scion Image software (Beta 4.02, 2000 Scion Corporation, freeware from the National Institutes of Health) was used to acquire and record antennule and aesthetasc structural parameters prior to antennulectomy and after the 1st, 2nd, and 3rd molts. After surgery and prior to the 1st molt, there was no external evidence of an antennule beyond a mound of scar tissue without any differentiated structure. Recorded measurements included antennule segment number, segment length, number of aesthetasc-bearing segments, aesthetasc length, aesthetasc diameter, distance between same-annulus aesthetasc rows (large gap), and distance between adjacent-annuli aesthetasc rows (short gap) (Fig. 2). The numbers of aesthetascs composing distal and proximal rows along the length of the aesthetasc-bearing region of the antennule were also recorded. Five measurements of each parameter per molt per animal were recorded in most cases, although difficulties due to mold placement or incomplete filling of the molds by the low viscosity resin occasionally led to fewer data points. Location along the antennule (distal, medial, proximal) was recorded except after the 1st molt, when the insufficiently developed structures made it difficult to identify positional landmarks. Only data from the middle portion of the aesthetasc-bearing region of the antennule were analyzed here, except in Figure 9.

Data analysis and statistics

The structural parameters were averaged for each molt for each animal, and then population means were calculated. One-way ANOVAs using regeneration stage as an independent variable, and Fisher's pair-wise least significant differences (PLSDs) were calculated using StatView software version 5.01 (SAS Institute). Chi-squared analysis for goodness of fit (calculated using Microsoft Excel 2003) was performed on the Y-maze data to determine variations in success rate across regeneration stages. A one-way ANOVA was used to analyze the differences among regeneration stages in the time needed to successfully complete the maze.

Results

Y-maze performance

Flicking and investigation of the substrate by both antennules (Fig. 3A) and Y-maze tracking ability in terms of both % success (Fig. 3B) and time to completion (Fig. 3C) were not fully restored until after the 3rd molt. Crayfish successfully chose the odor-containing arm of the Y-maze 79% of the time before antennulectomy (26/33 trials, $\chi^2_{\text{Original}} = 5.47$, $P < 0.05$), but not after antennulectomy (28% of the time, 5/18 trials, $\chi^2_{\text{0th}} = 1.78$, $P > 0.10$) or after the 1st (13/27 trials, 48% of the time, $\chi^2_{\text{1st}} = 0.02$, $P > 0.75$) or 2nd molt (8/14 trials, 57% of the time, $\chi^2_{\text{2nd}} = 0.14$, $P > 0.50$). After the 3rd molt, crayfish successfully chose the odor-containing arm 76% of the time (16/21 trials), significant at the 0.1 level ($\chi^2_{\text{3rd stage}} = 2.88$, $P < 0.10$) (Fig. 3B). Original, 2nd stage molt, and 3rd stage molt crayfish completed the task faster than 0th and 1st stage crayfish (Fig. 3C, ANOVA $F_{3,64} = 3.48$, $P < 0.05$). Most of this time was occupied by moving to the fork of the Y and choosing one side or the other; after a decision was made, the crayfish moved fairly swiftly to the end of the maze arm.

Antennule parameters

Figure 4 indicates that antennule length increased from 1.85 mm after the 1st molt to 4.90 mm by the 3rd molt, statistically indistinguishable from the original length of 4.95 mm (Fisher's PLSD, $P = 0.9125$). The average total number of antennule segments increased from 6.6 annuli after the 1st molt to 16.7 annuli after the 3rd molt (Fig. 5A), and the average number of segments bearing aesthetascs increased from 2.9 to 8.7 annuli (Fig. 5B) over the same series of molts, although both measurements were still slightly less than in the original antennule after the 3rd molt (average number of annuli before antennulectomy = 19.9 [Fisher's PLSD, $P = 0.020$]; average number of annuli with aesthetascs before antennulectomy = 10.6 [Fisher's PLSD, $P = 0.023$]). When the antennules regenerated, the newly formed segments were statistically indistinguishable from the original segments in length ($F_{3,41} = 0.726$, $P = 0.5424$, Fig. 6A). However, the relative spacing of the long gap (between aesthetasc rows on the same antennule segment) and the short gap (between aesthetasc rows on adjacent segments) did change as regeneration continued (Fig. 6B, C). Immediately after the 1st molt, the long gap was 25% shorter than in the original antennule (ANOVA, $F_{3,38} = 4.927$, $P = 0.0056$; Fig. 6B), and the short gap was 88% longer than in the original antennule (ANOVA, $F_{3,35} = 17.066$, $P < 0.0001$; Fig. 6C). By the end of the 3rd molt, the lengths of the long gap and the short gap were indistinguishable from their lengths in the pre-surgery antennule (Fisher's PLSD, $P = 0.7534$; Fisher's PLSD, $P = 0.8794$).

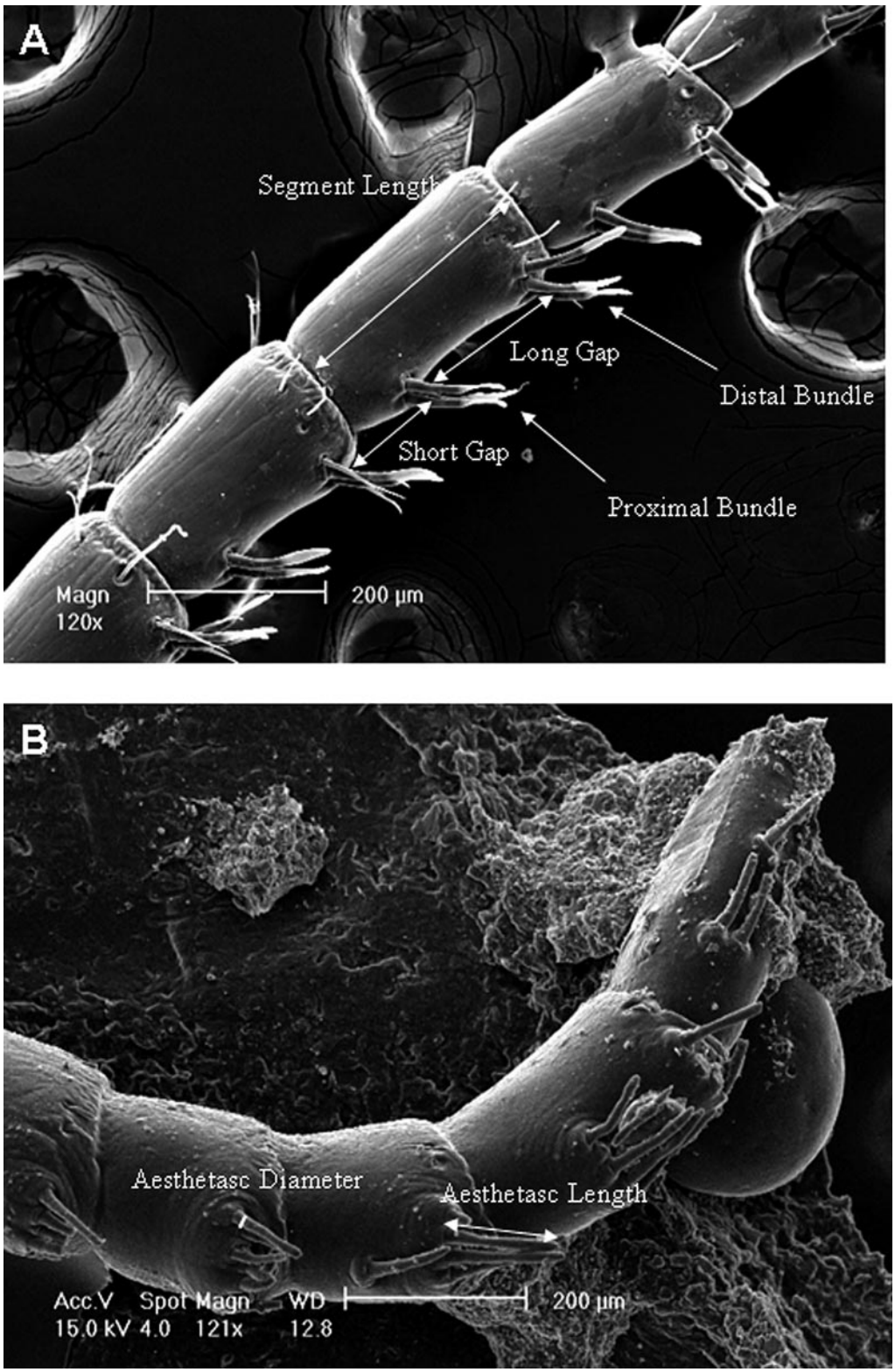

Figure 2. Scanning electron microscope images. (A) An original antennule. (B) A mold of a second-stage regenerating antennule.

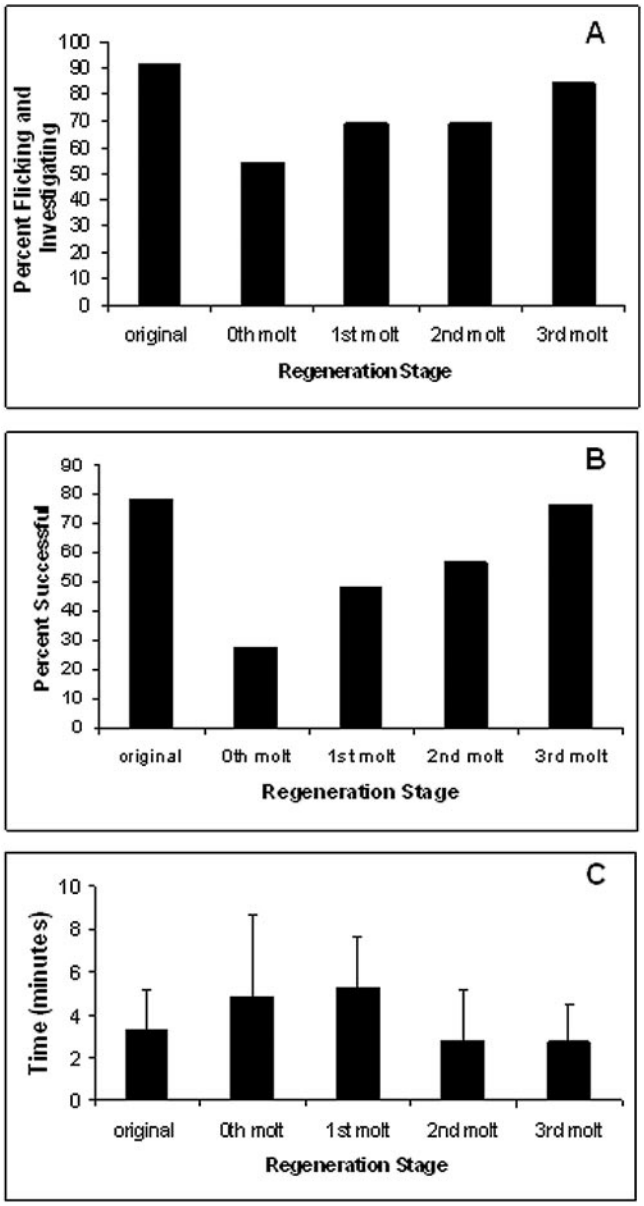

Figure 3. Y-maze test as a function of regeneration stage. (A) Percent of animals exhibiting flicking and investigative behavior when exposed to food odor in the Y-maze. Animals were tested once per molt stage: original ($n = 36$), pre-molt (0th molt) ($n = 33$), 1st molt ($n = 39$), 2nd molt ($n = 20$), 3rd molt ($n = 26$). By the 3rd molt, investigative behavior approached original values. (B) Success rate (% animals finding odor of the animals that make a decision). Animals were tested once per molt stage: original ($n = 33$), pre-molt (0th molt) ($n = 18$), 1st molt ($n = 27$), 2nd molt ($n = 14$), 3rd molt ($n = 21$). By the 3rd molt, success (76%, 16/21 trials, $\chi^2_{\text{3rd stage}} = 2.88$, $P < 0.10$) was equal to before the antennulectomy (79%, 26/33 trials, $\chi^2_{\text{Original}} = 5.47$, $P < 0.05$). (C) Time to complete Y-maze successfully decreases as a function of regeneration stage. Animals were tested once per molt stage; only times of successful animals are included here (means ± standard deviations): original ($n = 26$), pre-molt (0th molt) ($n = 5$), 1st molt ($n = 13$), 2nd molt ($n = 8$), 3rd molt ($n = 17$), ANOVA, $F_{3,64} = 3.48$, $P < 0.05$.

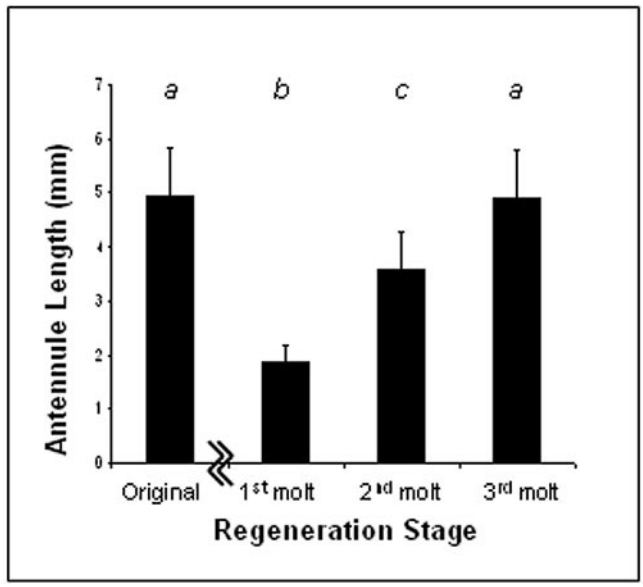

Figure 4. Antennule length as a function of regeneration stage. Data are means ± standard deviation. Numbers of animals measured are as follows: original ($n = 21$), 1st molt ($n = 7$), 2nd molt ($n = 13$), 3rd molt ($n = 3$). Different letters indicate significantly different means, ANOVA, $F_{3,40} = 31.075$, $P < 0.0001$. Zig-zag indicates break (surgery and time until after first molt) between original and 1st molt stages.

Aesthetasc parameters

After the 1st molt, the new aesthetascs were about 90% of their original length, but overall there was no effect of regeneration stage on aesthetasc length ($F_{3,36} = 1.971$, $P = 0.14$; Fig. 7A). Fisher's PLSD values showed that by the 2nd molt, aesthetasc length was indistinguishable from the original length ($P = 0.208$). New aesthetascs grew in with diameters indistinguishable from the original antennule ($F_{3,37} = 0.473$, $P = 0.70$) (Fig. 7B).

Gap:diameter ratio

Immediately after the first molt, the long gap:diameter ratio in the mid region of the antennule was 22% less than in the original antennules, but it was statistically indistinguishable from the original value by the 2nd molt stage (Fig. 8A, Fisher's PLSD, $P = 0.918$). The short gap:diameter ratio of the middle antennule region almost doubled immediately after antennulectomy, but returned to its original value by the 3rd molt stage (Fig. 8B, Fisher's PLSD, $P = 0.4046$).

Pattern of aesthetasc insertion during regeneration

In typical development, aesthetascs are primarily born in the proximal zone and move distally along the antennule toward the senescence region as an animal molts. During regeneration, this pattern appears not to hold.

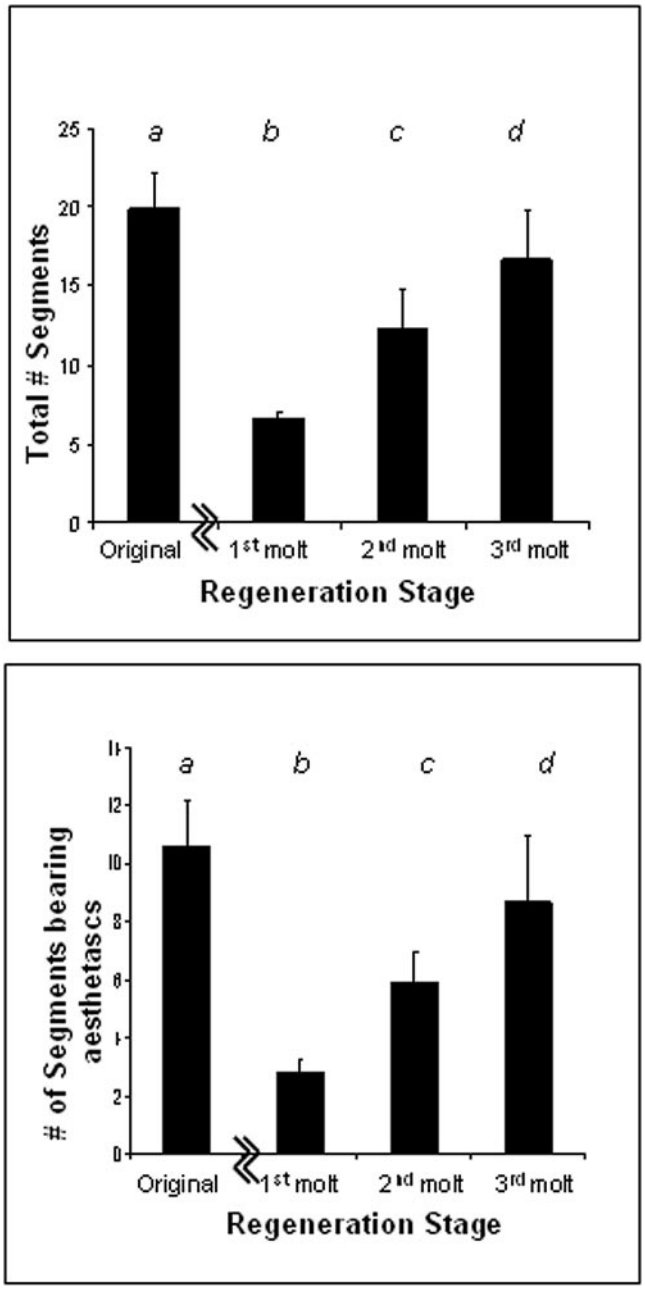

Figure 5. Antennule segments as a function of regeneration stage. (A) Total number of segments. (B) Number of segments bearing aesthetascs. Results shown are means ± standard deviation. Numbers of animals measured are as follows: original ($n = 21$), 1st molt ($n = 7$), 2nd molt ($n = 13$), 3rd molt ($n = 3$). All stages were significantly different; ANOVA, $F_{3,40} = 75.616$, $P < 0.0001$; ANOVA, $F_{3,40} = 70.268$, $P < 0.0001$. Zig-zag indicates break (surgery and time until after first molt) between original and 1st molt stages.

Figure 9 illustrates that by the 2nd molt, antennules exhibited more aesthetascs per segment along *all* regions of the antennule than in the 1st molt animals (ANOVA, Fisher PLSD, $P = 0.002$ for the distal region, 0.02 for the middle region, and 0.05 for the proximal region). It is unclear whether aesthetascs were shed as well as added between the 1st and 2nd regeneration stages, but it is certain that many more aesthetascs were added across all

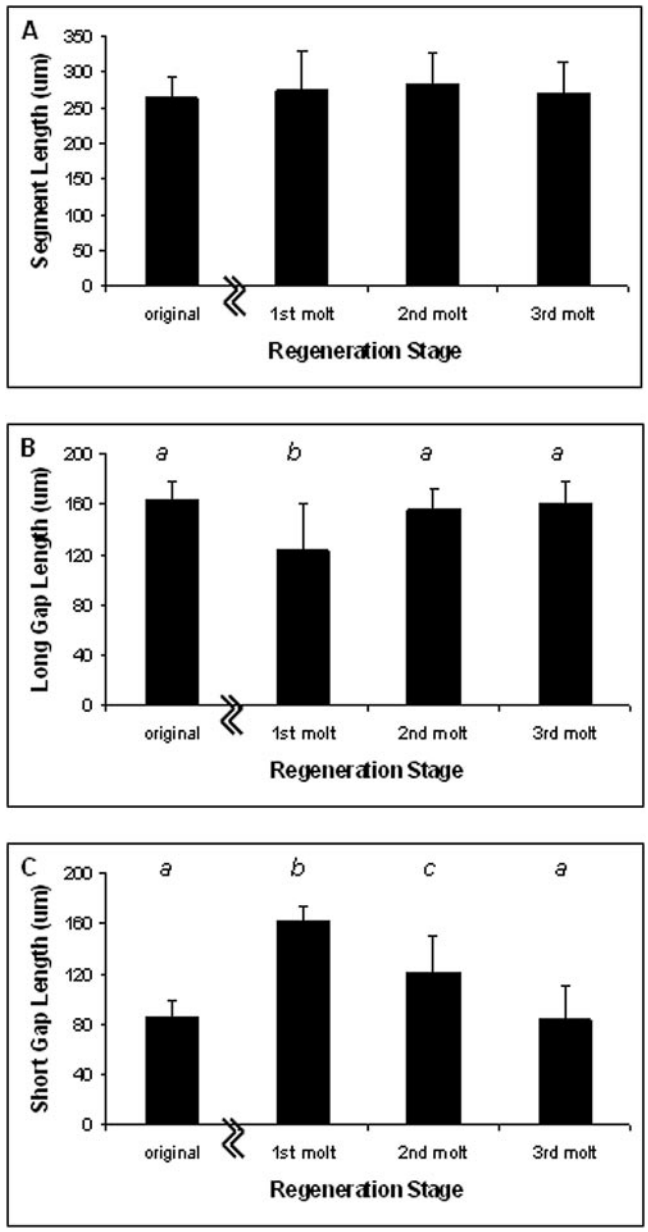

Figure 6. Segment length and gap lengths between adjacent aesthetasc rows as a function of regeneration stage. Results shown are means ± standard deviation. (A) Segment length did not change over the experiment, ANOVA, $F_{3,41} = 0.726$, $P = 0.5424$, $n = 21, 7, 14, 3$ for the four regeneration stages shown. (B) The long gap is the distance between adjacent rows of aesthetascs on the same segment. The 1st molt is significantly different from the others, ANOVA, $F_{3,38} = 4.927$, $P = 0.0056$, $n = 21, 4, 14, 3$ for the four stages shown. (C) The short gap is the distance between adjacent rows of aesthetascs on adjacent segments. All stages were significantly different, ANOVA, $F_{3,35} = 17.066$, $P < 0.0001$, $n = 21, 3, 13, 2$ for the four stages shown. Zig-zag indicates break (surgery and time until after first molt) between original and 1st molt stages.

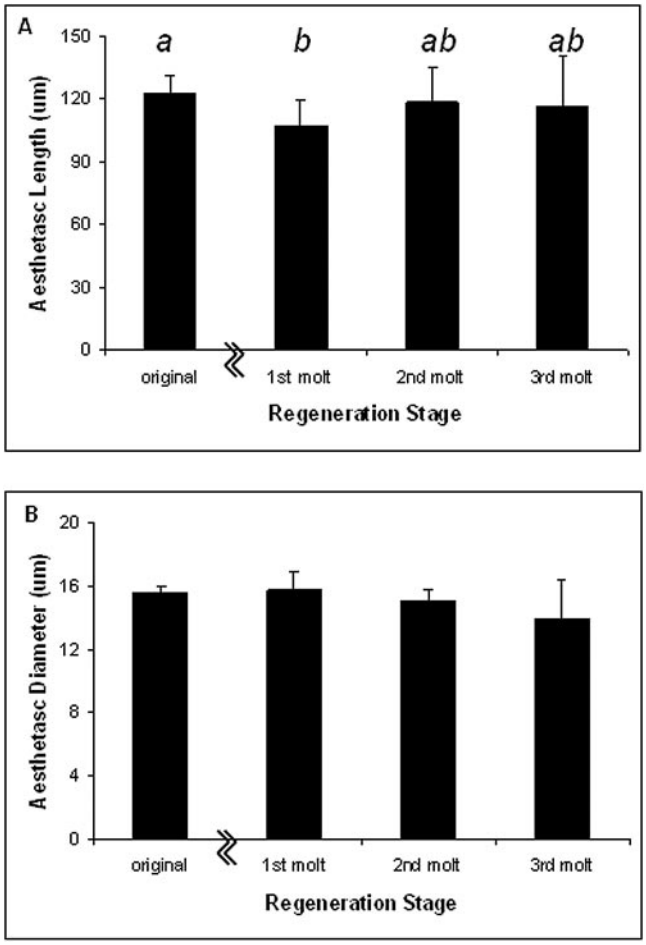

Figure 7. Aesthetasc length and diameter as a function of regeneration stage. (A) Aesthetascs are shorter after the first molt than pre-surgery (Fisher's PLSD, $P < 0.05$), but across all stages length does not vary with regeneration stage ($F_{3,36} = 1.971$, $P = 0.14$, $n = 21, 4, 13, 2$ for the four regeneration stages shown). (B) Aesthetasc diameter does not vary with regeneration stage ($F_{3,36} = 0.473$, $P = 0.70$, $n = 21, 4, 13, 2$ for the four regeneration stages shown). Data are means ± standard deviation. Zig-zag indicates break (surgery and time until after first molt) between original and 1st molt stages.

regions of the antennule than is observed in a normally developing adult individual.

Discussion

This project demonstrates a novel method for nondestructively studying regeneration in crayfish. Many of the changes over successive molts that we observed would not have been as apparent if we had not been able to repeatedly sample the same antennule on the same animals.

Hydrodynamic relevance of observed structural changes

As shown in Figure 3, the ability of *Orconectes sanborni* to successfully complete the Y-maze was significantly reduced by of the removal of a single antennule. Flicking and investigation of the substrate (Fig. 3A) and Y-maze odor-tracking ability in terms of both percent success (Fig. 3B) and time to completion (Fig. 3C) were not fully restored until after the 3rd molt. This indicated that the third-stage antennules had the architecture, the flicking patterns, or both necessary for effective olfaction. By identifying structural features that were altered between the 1st and 3rd molts, it may be possible to see which specific aspects of antennule and aesthetasc structure are critical for success.

Changes in antennule length, aesthetasc number, and length during regeneration

Most structural features had regained pre-antennulectomy form by the 2nd molt. We found that the antennule length, total number of segments, and number of segments with aesthetascs increased during regeneration. In addition, the number of aesthetascs per segment increased with regeneration stage (Fig. 9). Between the doubling of segments with

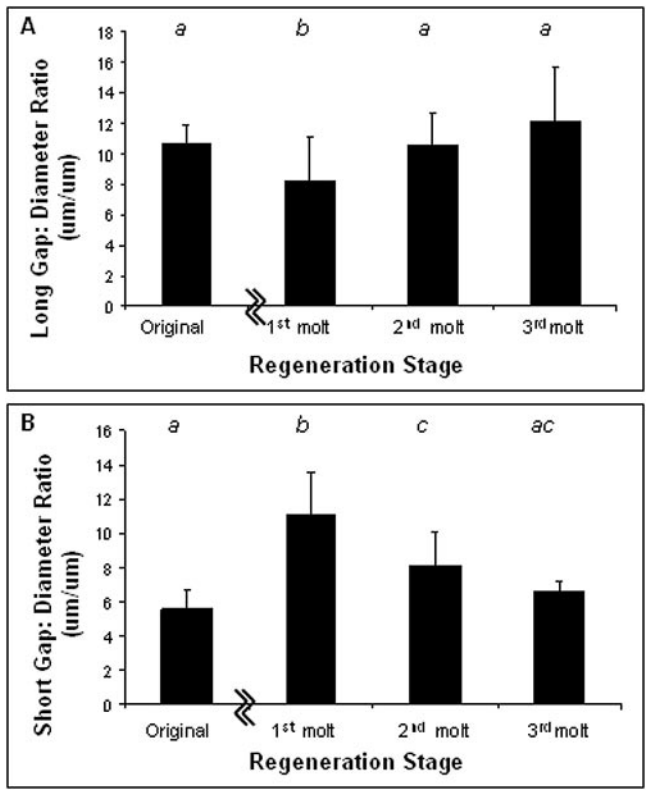

Figure 8. Gap:diameter ratio as a function of regeneration stage. (A) The long gap was statistically indistinguishable from the original value by the 2nd molt stage (Fisher's PLSD, $P = 0.918$). (B) The short gap:diameter ratio of the middle antennule region almost doubled immediately after antennulectomy, but returned to its original length by the 3rd molt stage (Fisher's PLSD, $P = 0.4046$). Mean ratio shown ± standard deviation, $n = 21, 7, 14, 3$ for the four regeneration stages shown. Zig-zag indicates break (surgery and time until after first molt) between original and 1st molt stages.

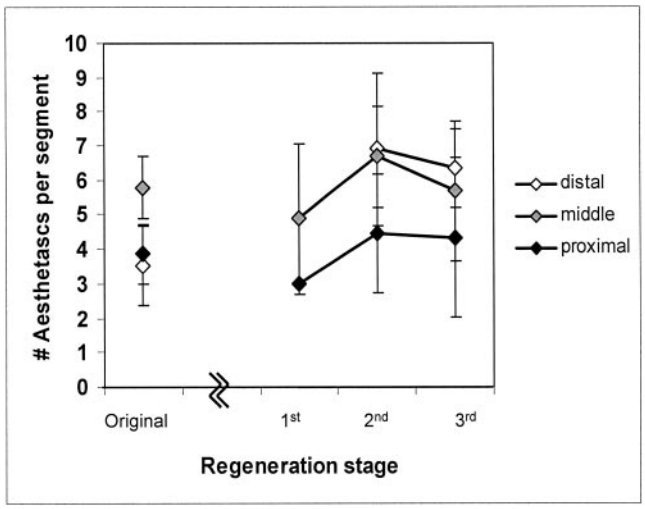

Figure 9. Number of aesthetascs per segment as a function of regeneration stage. 2nd molt antennules exhibited more aesthetascs per segment along all regions of the antennule than in 1st molt animals (ANOVA, Fisher PLSD, $P = 0.002$ for the distal region, $P = 0.02$ for the middle region, $P = 0.05$ for the proximal region. Data are means $\pm$ standard deviation, $n = 21, 4, 14, 3$ for the four stages shown. White, grey, and black diamonds indicate data from segments in the distal, middle, and proximal regions of the antennule. Zig-zag indicates break (surgery and time until after first molt) between original and 1st molt stages.

aesthetascs and the 40% increase in aesthetascs per segment, there was a 3-fold increase in the number of aesthetascs between the 1st and 2nd molt. In addition, the aesthetascs of the 2nd molt were 10% longer than those present after the 1st molt, and thus better able to extend beyond the boundary layer created by the supporting flagellum. The greater the amount of sensilla area able to sample the surrounding fluid, the more likely foraging, mate finding, predator avoidance, and localizing suitable habitat are to be effective. There was no statistically significant increase in sensilla number, length, or area between the 2nd and 3rd molts.

Segment length and spacing of aesthetasc rows

Although one strategy for maximizing olfactory function might be to increase the number of sensilla as rapidly as possible, other factors, such as spacing of sensilla, may come into play. For a given antennule length, it is possible either to have many aesthetasc rows crowded closely together, or to have fewer aesthetasc rows arranged more spaciously. Modeling work with cylinders suggests that having the sensilla too close together can inhibit the sampling of new fluid by the sensors (Cheer and Koehl, 1987; Hansen and Tiselius, 1992; Koehl, 1995, 1996; Mead and Koehl, 2000; Stacey *et al.*, 2003). Sensilla that are far apart may favor rapid odor arrival at the sensillar surface, while sensilla close together may favor retention of the odor signal for longer, possibly allowing for more sensitive olfaction (Mead *et al.*, 1999; Mead and Koehl, 2000; Stacey *et al.*, 2003).

In normal adult *O. sanborni*, the two rows of aesthetascs are not spaced evenly. The gap between the rows is wider on the same segment (long gap) than on adjacent segments (short gap). One hypothesis for this arrangement is that the spacious arrangement of sensilla divided by the long gap could tend to facilitate rapid sampling, while the more crowded pattern of aesthetasc placement around the short gap could facilitate longer retention of odors. This speculation will have to be tested with dynamically scaled physical models of antennules.

Although segment length remained roughly constant as new segments were added during regeneration, the positions of the proximal and distal aesthetasc rows changed, affecting the relative sizes of the small and large gaps (and the small and large gap:diameter ratios). After the 1st molt, the long gap:diameter ratio was smaller than normal, and the short gap:diameter ratio was larger than usual. By the second molt, the gap:diameter ratios had returned to their original proportions. Because Y-maze results indicated that first-stage animals were less able to effectively decipher important chemical information from the fluid sample, the typical long gap:diameter and short gap:diameter ratios may be necessary as complementary systems for orientation and navigation behaviors.

Pattern of aesthetasc insertion during regeneration

In typical post-settlement crustacean development, each molt involves the addition of new aesthetascs at the proximal portion of the aesthetasc-bearing region and the shedding of the oldest aesthetascs from the distal-most region of the antennule (Mellon *et al.*, 1989; Sandeman and Sandeman, 1996). This same pattern holds true for cuticular articulated peg organ sensilla in rock lobsters, which are added proximally and are lost distally (Macmillan *et al.,* 1998). This similarity suggests that this ordered, sequential turnover of receptor elements may be a common theme in crustacean sensory systems. However, in crayfish less than 7 mm in carapace length, aesthetascs are added uniformly along the entire aesthetasc-bearing portion of the antennule (Sandeman and Sandeman, 1996). This latter pattern was observed in these experiments post-surgery, although the crayfish were 2–6 cm in length: more aesthetascs were added across all regions of the antennule than is observed in a normally developing adult individual.

It should be noted that although one antennule was untreated and the structural features of the regenerating antennule were intact by the end of the 2nd molt, Y-maze success did not regain pre-antennulectomy levels until after the 3rd molt. We hypothesize that this discrepancy is due to features of odor-sampling movements ("flicks") that may not be in

place until after the 3rd molt. Possible flicking parameters that could affect sampling success are antennule velocity, Reynolds number, leakiness describing flow around aesthetascs during flicking, and symmetry of the flick. Changes in these features would not necessarily be reflected in aesthetasc structure but could affect olfactory sampling and thus odor-tracking. This is currently under investigation.

It should also be noted that this project focuses on correlating changes in aesthetasc structure and spacing with Y-maze success. Non-aesthetasc chemosensory setae on the antennule may contribute to tracking of food odors. Candidate setae that may have chemosensory function and may be associated with the non-aesthetasc pathway appear to be smaller and less numerous than aesthetascs, but they are closely associated with the aesthetascs. Therefore, we hypothesize that some of the same patterns of changes in aesthetasc spacing will hold for these non-aesthetasc chemosensory setae as well. Changes in these setae as a function of regeneration stage are under investigation.

Acknowledgments

We thank the Denison University Research Foundation and the Denison University Provost's Office for providing funds to conduct this project; Eric Liebl and Nestor Matthews for their helpful comments; Whitney Stocker for general crayfish expertise; Brian Kemmenoe and Kathy Wolken at the Ohio State University Campus Microscopy and Imaging Facility for technical assistance; the Denison University library staff for bibliographic assistance; and Charles Derby and three anonymous reviewers for helpful comments.

Literature Cited

Ache, B. W. 1982. Chemoreception and thermoreception. Pp. 369–393 in *The Biology of Crustacea*, Vol. 3, H. L. Atwood and D. C. Sandeman, eds. Academic Press, New York,

Breithaupt, T. 2001. Fan organs of crayfish enhance chemical information flow. *Biol. Bull*. **200:** 150–154.

Cheer, A. Y. L., and M. A. R. Koehl. 1987. Paddles and rakes: fluid flow through bristled appendages of small organisms. *J. Theor. Biol.* **129:** 17–39.

Derby, C. D., H. S. Cate, P. Steullet, and P. J. H. Harrison. 2003. Comparison of turnover in the olfactory organ of early juvenile stage and adult Caribbean spiny lobsters. *Arth. Struct. Dev*. **31:** 297–311.

Devine, D. V., and J. Atema. 1982. Function of chemoreceptor organs in spatial orientation of the lobster, *Homarus americanus*: differences and overlap. *Biol. Bull*. **163:** 144–153.

Dunham, D. W., K. A. Ciruna, and H. H. Harvey. 1997. Chemosensory role of antennules in the behavioral integration of feeding by the crayfish *Cambarus bartonii*. *J. Crustac. Biol.* **17:** 27–32.

Geisler, M., J. Nadeau, and F. D. Sack. 2000. Oriented asymmetric divisions that generate the stomatal spacing pattern in *Arabidopsis* are disrupted by the *too many mouths* mutation. *Plant Cell* **12:** 2075–2086.

Giri, T., and D. W. Dunham. 1999. Use of the inner antennule ramus in the localisation of distant food odours by *Procambarus clarkii* (Girard, 1852) (Decapoda, Cambaridae). *Crustaceana* **72:** 123–127.

Gleeson, R. A. 1982. Morphological and behavioral identification of the sensory structures mediating pheromone reception in the blue crab, *Callinectes sapidus. Biol. Bull.* **163:** 162–171.

Gleeson, R. A., W. E. S. Carr, and H. G. Trapido-Rosenthal. 1993. Morphological characteristics facilitating stimulus access and removal in the olfactory organ of the spiny lobster, *Panulirus argus*: insight from the design. *Chem. Senses* **18:** 67–75.

Gleeson, R. A., L. M. McDowell, and H. C. Aldrich. 1996. Structure of the aesthetasc (olfactory) sensilla of the blue crab, *Callinectes sapidus*: transformations as a function of salinity. *Cell Tissue Res.* **284:** 279–288.

Hallberg, E., K. U. I. Johansson, and R. Elofsson. 1992. The aesthetasc concept: structural variations of putative olfactory receptor cell complexes in Crustacea. *Microsc. Res. Techniq*. **22:** 325–335.

Hallberg, E., K. U. I. Johansson, and R. Wallén. 1997. Olfactory sensilla in crustaceans: morphology, sexual dimorphism, and distribution patterns. *Int. J. Insect Morphol. Embryol.* **26:** 173–180.

Hansen, B., and P. Tiselius. 1992. Flow through the feeding structures of suspension feeding zooplankton: a physical model approach. *J. Plankton Res.* **14:** 821–834.

Harrison, P. J. H., H. S. Cate, E. S. Swanson, and C. D. Derby. 2001. Postembryonic proliferation in the spiny lobster antennular epithelium: rate of genesis of olfactory receptor neurons is dependent on molt stage. *J. Neurobiol.* **47:** 51–66.

Harrison, P. J. H., H. S. Cate, P. Steullet, and C. D. Derby. 2003. Amputation-induced activity of progenitor cells leads to rapid regeneration of olfactory tissue in lobsters. *J. Neurobiol.* **55:** 97–114.

Harrison, P. J. H., H. S. Cate, and C. D. Derby. 2004. Localized ablation of olfactory receptor neurons induces both localized regeneration and widespread replacement of neurons in spiny lobsters. *J. Comp. Neurol.* **471:** 72–84.

Horner, A. J., M. Schmidt, D. H. Edwards, and C. D. Derby. 2008. Role of the olfactory pathway in agonistic behavior of crayfish *Procambarus clarkii. Invertebr. Neurosci* **8:** 11–18.

Horner, A. J., M. J. Weissburg, and C. D. Derby. 2004. Dual antennular pathways can mediate orientation by Caribbean spiny lobsters in naturalistic flow conditions. *J. Exp. Biol.* **207:** 3785–3796.

Koehl, M. A. R. 1995. Fluid flow through hair-bearing appendages: feeding, smelling, and swimming at low and intermediate Reynolds numbers. Pp. 157–182 in *Biological Fluid Dynamics,* C. P. Ellington and T. J. Pedley, eds.. *Symp. Soc. Exp. Biol.* No. 49.

Koehl, M. A. R. 1996. When does morphology matter? *Annu. Rev. Ecol. Syst.* **27:** 501–542.

Kraus-Epley, K. E., and P. A. Moore. 2002. Bilateral and unilateral antennal lesions alter orientation abilities of the crayfish, *Orconectes rusticus*. *Chem. Senses* **27:** 49–55.

Laverack, M. S. 1988. The numbers of neurons in decapod Crustacea. *J. Crustac. Biol.*. **8:** 1–11.

McMillan, D. L., T. Stuart, and M. Thomas. 1998. Development of a proprioceptive organ on the walking legs of the rock lobster *Jasus edwardsii* (Decapods: Palinuridae) by ordered addition and loss of receptor elements. *J. Crustac. Biol.* **18:** 1–9.

Mead, K., and M. A. R. Koehl. 2000. Stomatopod antennule design: the asymmetry, sampling efficiency, and ontogeny of olfactory flicking. *J. Exp. Biol.* **203:** 3795–3808.

Mead, K., M. A. R. Koehl, and M. O'Donnell. 1999. Stomatopod sniffing: the scaling of chemosensory sensilla and flicking behavior with body size. *J. Exp. Mar. Biol. Ecol.* **241:** 235–261.

Mellon, D. 2000. Convergence of multimodal sensory input onto higher-level neurons of the crayfish olfactory pathway. *J. Neurophysiol.* **84:** 3043–3055.

Mellon, D., Jr. 2007. Combining dissimilar senses: central processing of hydrodynamic and chemosensory inputs in aquatic crustaceans. *Biol. Bull.* **213:** 1–11.

Mellon, D. F., H. R. Tuten, and J. Redick. 1989. Distribution of

radioactive leucine following uptake of olfactory sensory neurons in normal and heteromorphic antennules. *J. Comp. Neurol*. **280:** 645–662.

Sandeman, R., and D. Sandeman. 1991. Stages in the development of the embryo of the fresh-water crayfish *Cherax destructor*. *Roux's Arch. Dev. Biol*. **200:** 27–37.

Sandeman, R., and D. Sandeman. 1996. Pre- and postembryonic development, growth and turnover of olfactory receptor neurones in crayfish antennules. *J. Exp. Biol.* **199:** 2409–2418.

Schmidt, M., and B. W. Ache. 1992. Antennular projections to the midbrain of the spiny lobster. II. Sensory innervation of the olfactory lobe. *J. Comp. Neurol.* **319:** 291–303.

Schmidt, M., and B. W. Ache. 1996. Processing of antennular input in the brain of the spiny lobster, *Panulirus argus.* I. Non-olfactory chemosensory and mechanosensory pathways of the lateral and median neuropil. *J. Comp. Physiol. A* **178:** 579–604.

Schmidt, M., L. Van Eckeris, and B. W. Ache. 1992. Antennular projections to the midbrain of the spiny lobster. I. Sensory innervation of the lateral and medial antennular neuropils. *J. Comp. Neurol.* **318:** 277–290.

Schmitt, B.C., and B. W. Ache. 1979. Olfaction: responses of a decapod crustacean are enhanced by flicking. *Science* **205:** 204–206.

Skinner, D. M. 1982. Molting and regeneration. Pp. 43–146 in *The Biology of Crustacea*, Vol. 9, *Integument, Pigments, and Hormonal Processes,* D. E. Bliss and L. H. Mantel, eds. Academic Press, New York.

Snow, P. J. 1973. Ultrastructure of the aesthetasc hairs of the littoral decapod, *Paragrapsus gaimardii. Z. Zellforsch.* **138:** 489–502.

Stacey, M. T., K. S. Mead, and M. A. R. Koehl. 2003. Molecular capture by olfactory antennules: mantis shrimp. *J. Math. Biol.* **44:** 1–30.

Steullet, P., H. S. Cate, and C. D. Derby. 2000a. A spatiotemporal wave of turnover and functional maturation of olfactory receptor neurons in the spiny lobster *Panulirus argus*. *J. Neurosci*. **20:** 3282–3294.

Steullet, P., H. S. Cate, W. C. Michel, and C. D. Derby. 2000b. Functional units of a compound nose: aesthetasc sensilla house similar populations of olfactory receptor neurons on the crustacean antennule. *J. Comp. Neurol*. **418:** 270–280.

Steullet, P., O. Dudar, T. Flavus, M. Zhou, and C. D. Derby. 2001. Selective ablation of antennular sensilla on the Caribbean spiny lobster *Panulirus argus* suggests that dual antennular chemosensory pathways mediate odorant activation of searching and localization of food. *J. Exp. Biol*. **204:** 4259–4269.

Tierney, A. J., C. S. Thompson, and D. W. Dunham. 1986. Fine structure of aesthetasc chemoreceptors in the crayfish *Orconectes propinquus*. *Can. J. Zool.* **64:** 392–399.